Synthesis and Unexpected Reactivity of Iron Tris(bipyridine) Complexes with Poly(ethylene glycol) Macroligands

Anne Pfister and Cassandra L. Fraser*

Department of Chemistry, University of Virginia, McCormick Road, Post Office Box 400319, Charlottesville, Virginia 22904-4319

Received September 6, 2005; Revised Manuscript Received November 22, 2005

High molecular weight poly(ethylene glycol) (PEG) derivatized iron tris(bipyridine) complexes, presenting hydroxyl end groups for further modification as bioconjugates, copolymers, or cross-linking agents, were synthesized via ring-opening anionic polymerization of ethylene oxide from hydroxyl-functionalized bipyridine (bpy) initiators and subsequent chelation to iron(II). Bpy-centered PEG macroligands ($bpyPEG_2$) with molecular weights ranging from 4000 to 17 000 and low polydispersity indices (<1.1) were obtained. Chelation of the $bpyPEG_2$ macroligands to iron(II) sulfate was studied in aqueous solution by titration and kinetics experiments, which revealed unexpected air sensitivity compared to nonpolymeric iron tris(bipyridine) complexes. Red-violet aqueous solutions of $[Fe(bpyPEG_2)_3]^{2+}$ begin to bleach within hours when exposed to air. Enhanced polymer degradation and gel formation of acrylate-modified $bpyPEG_2$ in the presence of Fe^{2+} suggest that radicals may be involved. Under argon, the chromophores are stable. Polymeric iron complexes are slower to form and faster to degrade in air with increasing $bpyPEG_2$ molecular weight. These studies demonstrate the influence of molecular weight in polymeric iron tris(bipyridine) complex coordination chemistry and reactivity.

Introduction

There is growing interest in metal complexes for use as molecular probes, sensors, imaging agents, and therapeutics. Many biomedical applications benefit from the incorporation of metals into polymers, which can enhance solubility, circulation time, and bioavailability, decrease toxicity, and serve as a platform for multifunctional systems incorporating drug loading, targeting, imaging, and degradation capabilities.

Metal coordinate bonds are often exploited as responsive structural motifs in polymer architectures and can lend unique reactivity to biomaterials.[1] Polymeric metal complexes are a specific class of macromolecules in which metals appear as a single well-defined cross-link at the center of linear or star-shaped materials (e.g., Figure 1).[2,3] Other elaborate inorganic−organic hybrid materials[4−6] are achievable through the introduction of reactive functional groups,[7] hydrogen-bonding associations,[8] sol−gel techniques,[9] additional metal binding sites,[10−11] or biological recognition.[12] Physical "cross-links" such as those that occur between dissimilar segments in block copolymers,[13−15] other kinds of nanoscale self-assembly,[16] and biopolymer secondary structures (DNA,[17] peptide nucleic acid,[18] or peptides[19]) represent additional levels of order and complexity.[20] Though metals often function as inert structural elements in macromolecular architectures, other times they are labile and responsive to physical or chemical features of the environment. This is useful in both the preparation and applications of metal-containing materials. Metal template/demetalation sequences have been employed in the synthesis of macroligands[21] and their nanoscale assemblies.[14] Sensitivity to temperature,[22] shear stress,[23] pH,[24] oxygen,[25] solvents and other analytes,[26] along with accompanying spectroscopic, magnetic, or other detectable changes, are often exploited for metal-based sensors,[27] molecular probes, and imaging agents.

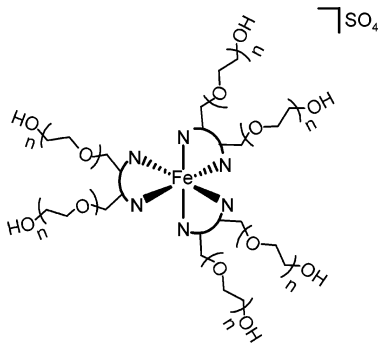

Figure 1. Schematic representation of iron-centered star-shaped poly(ethylene glycol), $[Fe(bpyPEG_2)_3](SO_4)$, showing hydroxyl chain ends.

In order for polymeric metal complexes to be useful building blocks in biological contexts, water-soluble and biocompatible systems are needed. Bipyridine-centered poly(ethylene glycol) (PEG) macroligands, $bpyPEG_2$, were targeted to meet both of these criteria. Bipyridine is a common bidentate ligand in coordination chemistry[28] and polymeric metal complex research, whereas PEG is a ubiquitous biocompatible material[29] found in protein nonadhesive surface coatings,[30] drug delivery systems[31] (e.g., stealth liposomes[32]), and hydrogels for tissue engineering.[33] Bioconjugates of PEG are also plentiful in targeting, recognition, and cell adhesion contexts.[34] Previously, PEG macroligands have been prepared by coupling methods. For example, bipyridine (bpy),[35] terpyridine (terpy),[11,36] and other ligands[10] have been modified with electrophilic functional groups (e.g., halides, acid chlorides) for reaction with hydroxyl or other nucleophilic termini on PEG. These preparations often require heterodifunctional PEGs, A−PEG−B, with one end rendered inert to coupling, if oligomeric byproducts and often difficult separations are to be avoided.[34,37] As a way around these molecular weight limitations and purification challenges, in this study we explore an alternative route to bipyridine-

* To whom correspondence should be addressed: e-mail fraser@virginia.edu.

10.1021/bm050652l CCC: $33.50
Published on Web 01/27/2006

centered PEGs, namely, anionic polymerization of ethylene oxide with 4,4′-bis(hydroxymethyl)-2,2′-bipyridine as the initiator and potassium naphthalenide as the base. An added benefit of this approach is that the chain ends of the resulting $bpyPEG_2$ feature hydroxyl groups, which can be further elaborated with bioconjugates, acrylates, or additional blocks. In this way, hydrogel networks and aqueous assemblies incorporating multiple kinds of cross-links—metal coordinate, physical, covalent, biological—can be generated. Such responsive materials are sensitive to multiple environmental parameters and capable of stepwise degradation, which is of interest for drug delivery and other uses of degradable biomaterials.[38−40]

As a starting point for metal-containing PEG biomaterials, we explore the iron(II) coordination chemistry of $bpyPEG_2$ macroligands (Figure 1). Detailed titration and kinetics studies verify the quality of the $bpyPEG_2$ macroligands and provide valuable information about the formation and stability of the resulting $[Fe(bpyPEG_2)_3]^{2+}$ complexes relative to nonpolymeric bpy analogues in the absence and presence of PEG. The aqueous chemistry of $[Fe(bpy)_3]^{2+}$ is well documented,[41] as are the preparations of polymeric iron tris(bpy) complexes with various homopolymer[3,42,43] and block copolymer compositions,[44] allowing for ready comparison. Iron is a common metal in biological systems, exhibiting reactivity ranging from radical generation and redox processes to oxygen binding, transport, and activation.[45] Furthermore, analogous to cytochrome P450 in the liver, polymer-supported iron tris(bpy) complexes have been utilized to activate oxygen and degrade organic contaminants in vitro,[46−48] thus demonstrating an additional role for polymeric $[Fe(bpy)_3]^{2+}$ materials. The extent to which iron bpy PEG complexes behave similarly and can be harnessed for therapeutic or environmentally beneficial purposes is an important avenue for investigation.

Experimental Section

Materials. The difunctional ligand initiator 4,4′-bis(hydroxymethyl)-2,2′-bipyridine ($bpy(CH_2OH)_2$)[49] and $[Fe(bpy)_3]SO_4$[50] were synthesized by previously reported procedures. Condensed ethylene oxide (EO) (CAUTION, Aldrich) was dried over calcium hydride (3×) and stored in a Kontes flask. The macroligands $bpy(CH_2OPEGOCH_3)_2$[51] and $bpy(C(O)OPEGOCH_3)_2$[35] were synthesized by coupling reactions as previously reported. Tetrahydrofuran (THF) was dried and purified by distillation over sodium/benzophenone or by passage through alumina columns.[52] Potassium naphthalenide was prepared by reaction of potassium and naphthalene in THF and titrated (3×) with a standardized HCl solution.[53] Iron sulfate heptahydrate was purchased from Strem Chemicals. HPLC-grade water (pH ∼6.5) was used for the titration and kinetics experiments with Fe(II). All other materials were obtained from Aldrich and used as received.

Methods. ^{1}H NMR (300 MHz) spectra were recorded on a Varian UnityInova 300 instrument in $CDCl_3$ and referenced to the signal for residual protiochloroform at 7.26 ppm. Molecular weights and polydispersity indices were determined by GPC in THF (20 °C; flow rate 1 mL/min) using Polymer Labs 5 μm mixed-C columns, a Hewlett-Packard 1100 instrument equipped with a laser refractometer LR40 (Viscotek), and Viscotek software (TriSEC GPC Version 3.0, Viscotek Corp.). Poly(ethylene glycol) standards (Polymer Laboratories) were used for molecular weight calibration. Samples were dissolved in THF (0.4% w/v) and passed through a 0.2 μm filter before injection. UV−vis spectra were recorded on a Hewlett-Packard 8453 diode-array spectrophotometer monitored by Biochemical Analysis UV−Vis software (Agilent) for solutions in Hellma sealable cuvettes with Fisher Teflon silicone septa.

$bpyPEG_2$ Synthesis. A representative procedure for samples prepared with 1:0.5 OH:base loading is described. $Bpy(CH_2OH)_2$ (0.086 g, 0.40 mmol) was dissolved in THF (3 mL) in a dry 25 mL Kontes flask under a nitrogen atmosphere. Potassium naphthalenide (1.5 mL of a 0.26 M solution, 0.40 mmol) was added dropwise, and the cloudy brown mixture was stirred for ∼1 h at room temperature. The reaction mixture was cooled to −78 °C and condensed EO (4 mL, 0.08 mol), first quantified in a dry graduated flask under nitrogen, was added by cannula transfer. The flask was sealed and the clear brownish solution was stirred at room temperature until the reaction mixture became solid (∼2 days). The reaction was vented, quenched with acidic methanol (0.5 mL of a stock solution composed of 1.5 mL of concentrated HCl in 25 mL of methanol),[54] dissolved in CH_2Cl_2, and concentrated by rotary evaporation. The crude product was precipitated from CH_2Cl_2 into cold diethyl ether (∼−78 °C), filtered, and dried in vacuo to give an off-white solid. For further purification, the resulting product was redissolved in CH_2Cl_2, passed through a neutral alumina plug, concentrated by rotary evaporation, and then precipitated from CH_2Cl_2 into cold diethyl ether. The resulting white solid was collected by filtration and dried in vacuo: 2.78 g (73%). GPC: M_n = 11 600, M_w = 12 500, PDI = 1.08. ^{1}H NMR δ: 8.65 (br s, bpy H-6, H-6′), 8.32 (br s, bpy H-3, H-3′), 7.37 (br s, bpy H-5, H-5′), 4.67 (s, bpyCH_2), 3.65 (m, PEG CH_2CH_2).

Determination of Fe(II) Concentration in $FeSO_4$ Stock Solutions by Titration with Bipyridine. A 100 mL aqueous stock solution of $FeSO_4 \cdot 7H_2O$ (71.5 mg, 0.26 mmol, ∼2.6 mM) and a 25 mL aqueous solution of 2,2′-bipyridine (7.4 mg, 47.5 μmol, 1.9 mM) were prepared in volumetric flasks. A portion of the $FeSO_4$ stock solution (0.1 mL) was added to water (2.4 mL) in a UV cuvette (1 cm path length) and the resulting ∼0.1 mM iron sulfate solution was titrated with the 2,2′-bipyridine solution. After addition of each 2,2′-bipyridine aliquot (50−100 μL) to the cuvette, the absorbance was measured spectrophotometrically at λ_{max} = 522 nm (metal-to-ligand charge-transfer (MLCT) for $[Fe(bpy)_3]^{2+}$). (Note: smaller 50 μL aliquots were added near the end point). The absorbance was then corrected for dilution[55] and plotted versus the equivalents of 2,2′-bipyridine added. The end point (i.e., the intersection of the linear segments of the curve) was determined and the concentration of iron(II) in the stock solution was calculated: 3.02 mM. Iron stock solutions, freshly prepared and thus titrated for each experiment, were then used in titration and kinetics experiments of polymeric ligands described below.

Fe(II) Titration with $BpyPEG_2$. A representative procedure is described. Titrations with other $bpyPEG_2$ macroligands were run at comparable concentrations. A 90 μM solution of $FeSO_4$ was prepared in a UV cuvette (1 cm path length) by combining 0.1 mL of a pretitrated 2.24 mM $FeSO_4$ stock solution with 2.4 mL of water. An aqueous solution of $bpyPEG_2$ (7.7 mg, 1.90 μmol, M_n = 4100, PDI = 1.11) was prepared in a 1 mL volumetric flask ($[bpyPEG_2]_0$ = 1.9 mM) and 50−100 μL aliquots were added to the iron salt solution in the UV cuvette. (Note: smaller 50 μL aliquots were added near the end point of the titration.) After each aliquot addition, the solution was stirred until the absorbance reached a constant value (∼30 min). The absorbance was then corrected for dilution[55] and plotted versus the equivalents of macroligand added. The end point of the titration was determined from the intersection of the linear segments of the curve.

Fe(II) Titration with Bipyridine in the Presence of Linear PEG. This control reaction was performed as described above for the Fe(II) titration with $bpyPEG_2$ macroligand, except that an aqueous stock solution containing both poly(ethylene glycol) (M_n = 4600, 1.9 mM) and bipyridine (1.9 mM) was used in place of $bpyPEG_2$ to titrate Fe(II) ($[FeSO_4]_0$ = 90 μM; 2.5 mL in the cuvette).

Kinetics of $[Fe(bpyPEG_2)_3]^{2+}$ Formation and Degradation: (a) Ambient Atmosphere. A representative procedure is provided. All kinetics experiments were run at comparable concentrations. $BpyPEG_2$ (6.9 mg, 0.6 μmol, M_n = 11 600, PDI = 1.08) was dissolved in water (2.418 mL) in a 1-cm path length cuvette, and a fraction of the pretitrated iron(II) solution (82 μL, 0.2 μmol, 80 μM) was added (total volume = 2.5 mL; $[bpyPEG_2]_0 = 3[FeSO_4]_0$ = 240 μM). The cuvette was then sealed and the solution was stirred. The reaction was monitored

spectrophotometrically every 5 min for 1 h, and then every 30 min for ~1 day. Reactions performed in the dark were conducted in an analogous manner with the following exceptions. Solutions of $FeSO_4$ and $bpyPEG_2$ were prepared separately under light. Then light was strictly excluded, the two reagents were combined, and the reaction was monitored in the dark over time.

(b) Argon Atmosphere. Kinetics experiments were performed as described above with the exception that the solvent was purged with argon. The volumetric flask containing the iron salt and the UV cuvette containing the polymer were sealed, evacuated, and purged with argon (3×) before addition of the solvent with an argon-purged syringe. The reaction solution was stirred in a sealed cuvette and monitored every 5 min for 1 h and then every 30 min for 20 h. After this time, the cuvette cap was removed and the atmosphere above the solution was purged with air. After 20 min, the cuvette was resealed to prevent evaporation and the reaction was monitored every 30 min past the point where a minimum absorbance value was reached.

(c) Data Analysis and Curve Fitting. The kinetics traces were analyzed with IGOR PRO software (WaveMetrics). The rates of disappearance of $[Fe(bpyPEG_2)_3]^{2+}$ in the kinetics curves were fitted to the equation for a first-order reaction with an additional offset (A') because, typically, the absorbance did not reach zero over time: $A = A' + A_0e^{-kt}$, where A_0 = the absorbance at the decay onset, A' = the residual absorbance after decay, and k = the rate constant for the disappearance of $[Fe(bpyPEG_2)_3]^{2+}$. The measure of the quality of the fit is the least-squares residual sum (i.e., the χ^2 parameter).

Kinetics of $[Fe(bpy)_3]^{2+}$ Formation and Degradation in the Presence of PEG: (a) Ambient Atmosphere. Aqueous stock solutions of 2,2′-bipyridine (24.9 mg, 0.16 mmol) and PEG (15.9 mg, 3.46 μmol) were prepared in volumetric flasks (25 and 10 mL, respectively). 2,2′-Bipyridine (94 μL of stock solution, 0.6 μmol) and PEG (1736 μL of stock solution, 0.6 μmol) were combined in a 1-cm path length cuvette, and pretitrated iron(II) solution (71 μL, 0.2 μmol) and water (599 μL) were added (total volume = 2.5 mL; $[bpy]_0 = [PEG]_0 = 3[FeSO_4]_0$ = 240 μM). The cuvette was sealed, and the solution was stirred and monitored spectrophotometrically every 5 min for 1 h and then every 30 min for ~1 day.

(b) Argon Atmosphere. Kinetics experiments were performed as described above except that the solvent, the three volumetric flasks containing $FeSO_4$, bpy, and PEG, the UV cuvette, and the syringes used for solution transfer were purged with argon. The reaction solution under argon was stirred in a sealed cuvette and monitored every 5 min for 1 h and then every 30 min for 20 h. After this time, the cuvette cap was removed and the atmosphere above the solution was purged with air. After 20 min, the cuvette was resealed to prevent evaporation and the reaction was monitored every 30 min past the point where a minimum absorbance value was reached.

(c) Data Analysis and Curve Fitting. Data were analyzed as described above for $[Fe(bpyPEG_2)_3]^{2+}$.

$[Fe(bpyPEG_2)_3]SO_4$ Synthesis. Aqueous solutions of $FeSO_4$ (1 mL, 0.0108 M), prepared and stored under argon, and $bpyPEG_2$ (0.201 g, 0.032 mmol, M_n = 6200, PDI = 1.09) were combined in a 50 mL round-bottom flask and stirred for 45 min at room temperature. The red violet solution was dried in vacuo for 3 days on the Schlenk line to give a red solid: 0.202 g (99%). UV−vis (H_2O, air) MLCT λ_{max} (ϵ): 532 nm (8442 M^{-1} cm^{-1}). The solid was dissolved in a minimal amount of CH_2Cl_2 and precipitated into cold diethyl ether. The red-violet powder was collected by centrifugation, the solvent was decanted, and the product was dried in vacuo: 0.154 g (78%). UV−vis (H_2O, air) MLCT λ_{max} (ϵ): 531 nm (9420 M^{-1} cm^{-1}).

Results and Discussion

Macroligand Synthesis. The living anionic polymerization of ethylene oxide (EO) is initiated by activation of hydroxyl groups with bases.[53,54,56−58] Correspondingly, difunctional bpy-$(CH_2OH)_2$ was reacted with potassium naphthalenide (typically ~0.2−0.3 M) in a 1:1 hydroxyl:base ratio to generate alkoxide nucleophiles for reaction with EO in THF solution (eq 1).

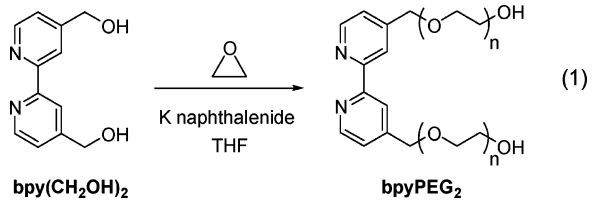

bpy(CH$_2$OH)$_2$ **bpyPEG$_2$** (1)

Reactions were stirred until the solution became viscous (1−2 days) and then were quenched with acidic methanol. The purification of the reaction mixture by precipitation from CH_2Cl_2/hexanes yielded polymers that were tan in color. Molecular weight data including polydispersity indices (PDIs) obtained by gel-permeation chromatography (GPC) in THF solution (vs PEG standards) are given in Table 1. As is illustrated in entries 1−5, for 1:1 hydroxyl:base loadings the PDIs are typically broad, ranging from 1.2 to 1.4, with some GPC traces exhibiting low molecular weight shoulders. Further purification of tan samples by filtration through neutral alumina and reprecipitation resulted in decolorized polymers with similar or slightly narrower molecular weight distributions at the expense of lower yields (e.g., Table 1, entry 3: before alumina, brownish, PDI = 1.16, yield = 92%; after alumina,: white, PDI = 1.16, yield = 60%).

Table 1. GPC Molecular Weight Data[a] for Representative $BpyPEG_2$ Macroligands

entry	OH:base:EO[b]	$[I]_0$[b] (mM)	$[EO]_0$[b] (M)	M_n calcd[c]	M_n	M_w/M_n
1[d]	1:1:35	65	4.6	6400	4400	1.33
2[d,e]	1:1:57	63	7.1	5200	5800	1.41
3[e]	1:1:112	34	7.6	10 200	9500	1.16
4	1:1:119	34	8.0	10 600	12 500	1.29
5	1:1:225	20	9.1	19 900	16 300	1.29
6	1:0.5:51	87	8.8	4700	6200	1.09
7	1:0.5:100	89	17.8	9100	11 600	1.08
8	1:0.5:200	53	21.2	17 800	17 400	1.08
9	1:0.35:49	128	12.5	4500	5300	1.10
10	1:0.35:226	81	36.4	20 200	14 300	1.08

[a] Determined in THF vs PEG standards with refractive index detection. [b] OH = one hydroxyl group of the difunctional initiator (I), $bpy(CH_2OH)_2$; base = potassium naphthalenide (0.2−0.3 M unless otherwise indicated); EO = ethylene oxide. [c] Determined from the monomer/initiator loading. [d] Precipitated twice from CH_2Cl_2/hexanes; not passed through an alumina plug. [e] [Potassium naphthalenide] = 1.14 M.

Previously it has been shown that the hydroxyl:base ratio can influence the molecular weight control that is observed in anionic polymerizations, particularly for multifunctional alkoxide initiators, which often exhibit limited solubility in common polymerization solvents. Low PDI materials have been attained with substoichiometric loadings of base.[56,57] In one approach, the hydroxyl initiator sites were titrated with base, with a slight green color noted at the end point.[54] With $bpy(CH_2OH)_2$ however, the heterogeneous reaction mixture changed from yellow to brown upon addition of ~0.4 equiv of base per OH group and no precise titration end point was evident. Thus, 1:0.5 and 1:0.35 hydroxyl:base loadings were explored in an attempt to optimize molecular weight control. Samples were purified by precipitation from CH_2Cl_2:Et_2O and passage through a plug of neutral alumina. As shown in Table 1 (entries 6−10), PDIs decrease (<1.1) for both of these lower loadings; however, low molecular weight shoulders are typically observed in GPC traces of macroligands made with 1:0.35 hydroxyl:base loadings. Low molecular weight byproducts are less pronounced for 1:0.5 hydroxyl:base ratio, as is illustrated in Figure 2 for samples of different molecular weights.

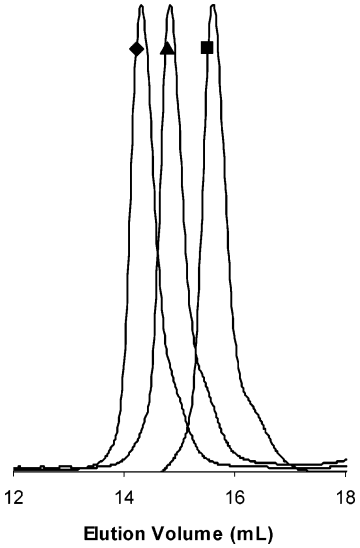

Figure 2. GPC traces (RI detection) of bpyPEG$_2$ macroligands prepared with a 1:0.5 initiator OH to base ratio. (■) M_n = 6200, PDI = 1.09; (▲) M_n = 11 600, PDI = 1.08; (◆) M_n = 17 400, PDI = 1.08. (Table 1, entries 6, 7, and 8, respectively).

^{1}H NMR spectral analysis of bpyPEG$_2$ products in $CDCl_3$ confirms that polymerization has initiated from both alcohol sites of bpy(CH_2OH)$_2$. Resonances corresponding to "benzylic" protons of the initiator, bpyCH_2OH, disappear, whereas new resonances associated with bpyCH_2OPEG appear at 4.67 ppm (compare to bpy(CH_2OH)(CH_2OPEGOMe): δ 4.82 and 4.68 ppm, respectively, in $CDCl_3$ solution).[51] For low molecular weight bpyPEG$_2$ macroligands, molecular weights determined by ^{1}H NMR show good correspondence with values obtained by GPC vs PEG standards [e.g., M_n GPC (NMR): 4400 (4100), 6200 (6500), 5300 (5800)]. For higher molecular weight bpyPEG$_2$ samples, bpy resonances are very small and broad relative to PEG -CH_2CH_2- peaks in the ^{1}H NMR spectra, rendering molecular weight determination by relative integration unreliable.

Polymeric Iron Complex Formation. In preliminary studies, the iron coordination chemistry of bpyPEG$_2$ (generated via 1:1 base:OH loading) was compared with that of other bpy macroligands based on poly(methyl methacrylate) (PMMA), poly(lactic acid) (PLA), poly(ϵ-caprolactone) (PCL), and polystyrene (PS) with bpy as a reference.[42] Extinction coefficients for the polymeric iron complexes were calculated from maximum absorbance values measured by UV−vis spectrophotometry, based on 3:1 bpy macroligand:iron(II) salt reagent loadings, with the assumption that the tris complex is the only species present in solution. Though this is not an accurate assumption for polydisperse polymer samples, especially those that do not form tris complex quantitatively, it nonetheless serves as a useful relative measure of the extent of reaction and/or quality of a given macroligand sample. Additionally, this corrects for any variations in concentration between experimental runs and allows for comparison of data obtained from different types of experiments.

With a 3:1 CH_2Cl_2/MeOH mixed solvent system to dissolve both [Fe(OH_2)$_6$](BF_4)$_2$ and the respective macroligands, the calculated molar extinction coefficients (ϵ) for iron bpyPEG$_2$ complexes were significantly smaller ($\epsilon \approx 4000$ M^{-1} cm^{-1}) than for [Fe(bpy)$_3$](BF_4)$_2$ ($\epsilon = 9450$ M^{-1} cm^{-1}) and other polymeric iron(II) tris(bipyridine) complexes of comparable and even significantly higher molecular weights.[42,59] (for example, compare to polymeric iron complexes prepared from bpyPLA$_2$: M_n = 6600, ϵ = 9860 M^{-1} cm^{-1}; M_n = 65 400, ϵ = 8129 M^{-1} cm^{-1}). This was true regardless of the bpyPEG$_2$ molecular weight (e.g., for M_n = 4100, ϵ = 4052 M^{-1} cm^{-1}; for M_n = 8600, ϵ = 4373 M^{-1} cm^{-1}; and for M_n = 16 800, ϵ = 4384 M^{-1} cm^{-1}) and the solvent system employed (e.g., for bpyPEG$_2$ M_n = 8600, in H_2O, ϵ = 3962 M^{-1} cm^{-1}; in CH_3OH, ϵ = 4519 M^{-1} cm^{-1}; and in CH_2Cl_2/MeOH, ϵ = 4373 M^{-1} cm^{-1}). Additionally, reaction times required to reach maximum absorbance at [Fe(bpyPEG$_2$)$_3$]$^{2+}$ MLCT ($\lambda_{max} \sim 532$ nm) were also extended for PEG relative to other polymers of comparable molecular weight (e.g., for bpyPEG$_2$, M_n = 8600, ~30 min; for bpyPS$_2$, M_n = 8400, ~5 min). To better understand this unique behavior observed for bpyPEG$_2$, titration and kinetics experiments were performed for macroligands of different molecular weights that were prepared and purified by various methods. Additionally, since the ultimate goal is to explore the potential of iron bpyPEG$_2$ complexes as biomaterials, it is important to understand their behavior in aqueous solution; thus, subsequent analytical and preparative reactions were run in H_2O and an iron salt with a more biocompatible counterion; namely, iron(II) sulfate heptahydrate, was adopted.

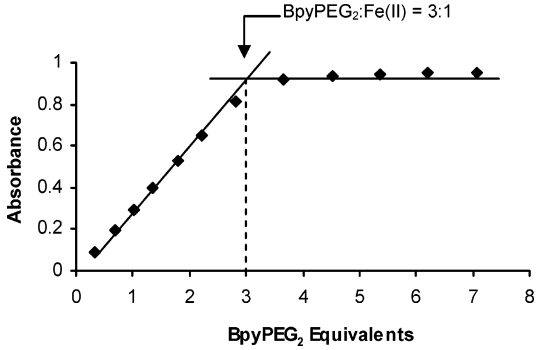

Figure 3. Titration plot for bpyPEG$_2$ (M_n = 5300, PDI = 1.10) with $FeSO_4$ in H_2O.

Iron(II) Titrations with BpyPEG$_2$. The quality and coordination chemistry of bpyPEG$_2$ macroligands were investigated by titration with iron. First, for each experiment, the metal concentrations in iron salt stock solutions were determined by titration with 2,2′-bipyridine (bpy), monitoring absorbance at λ_{max} (MLCT) = 522 nm. Iron salt solutions thus prepared and tested were subsequently used in titration experiments with bpyPEG$_2$ macroligands (Figure 3). Comparable initial concentrations of iron ([$FeSO_4$]$_0 \sim 90$ μM) and ligand stock solutions ([bpyPEG$_2$]$_0 \sim 1.9$ mM) were used in all titration experiments, and results from these studies are collected in Table 2.[60] As previously observed with other macroligands, the absorbances for [Fe(bpyPEG$_2$)$_3$]$^{2+}$ complexes are bathochromically shifted to λ_{max} (MLCT) ~532 nm (i.e., vs 522 nm for [Fe(bpy)$_3$]$^{2+}$).[42,44,59] In our earliest studies, more than 3 equivalents of bpyPEG$_2$ (and up to ~6 equivalents for certain samples) were required per equivalent of Fe(II) to reach the end point of the titration (Table 2, entries 1−3); whereas for polymeric bpy ligands based on PMMA, PLA, PCL, and PS, the end points were typically reached at macroligand-to-iron ratios of 3:1.[42] To better understand this unique behavior noted for bpyPEG$_2$, control reactions were run to determine whether donor groups on PEG (i.e., backbone ethers and/or alcohol end groups) can serve as effective competing ligands for bpy, as noted for other metal−polymer systems.[41,44,61] When Fe(II) was titrated with bpy in the presence of added PEG (Table 2, entry 5) under comparable conditions to bpyPEG$_2$ sample, 3 equivalents of bpy were necessary to reach the end point and the extinction coefficient was comparable to that of [Fe(bpy)$_3$]$^{2+}$ (Table 2, entry 4). Thus, when PEG and bpy are not covalently attached,

Table 2. Titration of Iron(II) Sulfate with $bpyPEG_2$ Macroligands Prepared and Purified by Different Methods[a]

entry	ligand	OH:base[b]	filtration[c]	M_n[d]	M_w/M_n[d]	$bpyPEG_2$:Fe(II)[e]
1	$bpyPEG_2$	1:1	none	4380	1.33	6.6:1
2	$bpyPEG_2$	1:1	alumina	4100	1.22	3.4:1
3	$bpyPEG_2$	1:1	alumina	9500	1.16	>5.2:1
4	bpy	NA[f]	NA	156	NA	3.0:1
5	bpy + PEG	NA	NA	4600	1.05	3.0:1
6	$bpy(PEGOCH_3)_2$	NA	none	4100	1.08	3.0:1
7	$bpy(C(O)OPEGOCH_3)_2$	NA	NA	4100	1.11	3.7:1
8a	$bpyPEG_2$	1:0.5	none	11 500	1.08	3.1:1
8b	$bpyPEG_2$	1:0.5	alumina	11 600	1.08	2.9:1
9a	$bpyPEG_2$	1:0.5	none	17 300	1.08	3.6:1
9b	$bpyPEG_2$	1:0.5	alumina	17 400	1.08	4.2:1
10a	$bpyPEG_2$	1:0.35	none	5100	1.14	4.3:1
10b	$bpyPEG_2$	1:0.35	silica	5200	1.13	3.3:1
10c	$bpyPEG_2$	1:0.35	alumina	5300	1.10	3.0:1

[a] Titrations were performed at $[FeSO_4]_0 \sim 90\ \mu M$; $[bpyPEG_2]_0 \sim 1.9$ mM stock solutions. Absorbances were monitored at λ_{max} (~532 nm for $bpyPEG_2$ complexes and 522 nm for bpy) and corrected for dilution. [b] Reagent loading for macroligand synthesis: OH = one hydroxyl group of the difunctional initiator $bpy(CH_2OH)_2$; base = potassium naphthalenide. [c] Solid support used in polymer purification. [d] Determined by GPC in THF versus PEG standards. [e] Reagent ratio at the end point of spectrophotometric titration. [f] Not applicable.

PEG backbone ethers and alcohol end groups did not interfere in a measurable way with the titration of Fe with bpy.

Another possible explanation for the >3:1 ratios observed for iron titrations with $bpyPEG_2$ pertains to the quality of the macroligand obtained by different synthetic methods. For example, samples with impurities or lower than expected bpy content could also lead to elevated macroligand-to-iron ratios in titrations. To test these possibilities, $bpyPEG_2$ macroligands generated by different methods and base loadings that were purified by various filtration and precipitation procedures were employed in iron titration experiments. Indeed, metal titration (i.e., polymer end-group analysis) serves as a useful probe of the quality of a macroligand sample and thus is helpful in optimizing polymerization conditions. For example, $bpyPEG_2$ samples prepared by ring-opening anionic polymerization with a 1:1 hydroxyl:base loading exhibited >3:1 $bpyPEG_2$:Fe^{2+} ratios at the titration end points regardless of molecular weight (Table 2, entries 1−3). In contrast, lower base loadings and purification by passage through alumina correlated with the 3:1 $bpyPEG_2$:Fe^{2+} ratio expected for high-quality samples (Table 2, entry 10c). By use of an alternative synthetic method, macroligands prepared by coupling bpy to PEG via ester linkages gave rise to a 3.7:1 ratio in titration experiments, suggesting the need for greater optimization in synthesis or purification (Table 2, entry 7). Note, however, that when PEG was coupled to $bpy(CH_2Cl)_2$ via ether linkages, a 3:1 macroligand-to-iron ratio was obtained (Table 2, entry 6). These observations with high-quality samples made via either anionic or coupling methods suggest that even when PEG is covalently attached to bpy, it does not effectively compete with bpy for iron(II) binding; ultimately polymeric iron tris(bpy) complexes form efficiently even when a bpy−PEG chelate effect is operative. For a higher molecular weight $bpyPEG_2$ sample (M_n = 17 400; Table 2, entry 9b), in contrast, greater than 3 equivalents of macroligand were needed to reach the end point of the iron titration even when the optimal method was used for synthesis and purification. Though further refinement of the synthetic methods may still be merited (e.g., through the use of a crown ether to activate the anion or a more polar solvent such as dimethyl sulfoxide, DMSO, provided that chain transfer is negligible),[56,57] this also points to a possible molecular weight effect on chelation, as has been noted previously for several polymer systems.[42,44,59,62] Equilibria may not be shifted entirely toward iron tris(bpy) products for higher molecular weight macroligands, or alternatively, as the kinetics studies discussed below indicate, polymeric metal complexes of different molecular weights exhibit different rates of formation and stabilities once formed.

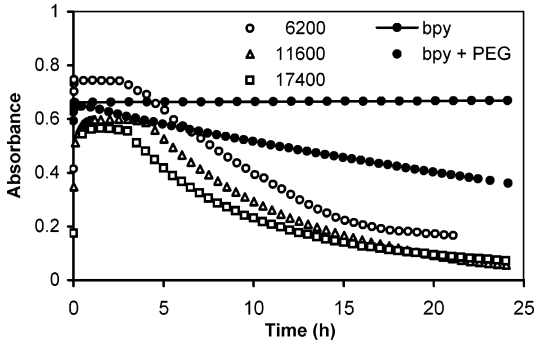

Figure 4. Rate comparison of $[Fe(bpyPEG_2)_3](SO_4)$ complex formation and degradation in water under ambient atmosphere for samples prepared from $bpyPEG_2$ macroligands of different molecular weights (M_n = 6200, 11 600, and 17 400). Data for the formation and degradation of $[Fe(bpy)_3](SO_4)$ in the absence and presence of PEG (M_n = 4600) are provided for comparison. ($[FeSO_4]_0 = {}^1/_3[\text{bpy ligand}]_0 = 80\ \mu M$; absorbance changes are monitored at MLCT $\lambda_{max} \sim 532$ nm for the $bpyPEG_2$ macroligands and 522 nm for bpy). See Figure 5 for the corresponding UV−vis spectra for the iron complex of $bpyPEG_2$ (M_n = 6200) monitored over time.

Kinetics of $[Fe(bpyPEG_2)_3]^{2+}$ Formation and Degradation. Initially, kinetics experiments were performed at 3:1 $bpyPEG_2$ to Fe^{2+} loadings to compare the rates and extent of iron tris($bpyPEG_2$) complex formation for macroligands of different molecular weights. It was subsequently noted, however, that iron tris($bpyPEG_2$) complexes decompose over time. This behavior is in marked contrast to $[Fe(bpy)_3](SO_4)$,[41,63] which forms readily and is stable in water under air (Figure 4).[64] If formation and decomposition occur concurrently during the course of preparative reactions or titration experiments with polymeric ligands, then this could account for the depressed extinction coefficients and elevated macroligand-to-metal ratios that are observed in titrations with $bpyPEG_2$.

To further explore this unexpected reactivity, kinetics experiments with 3:1 $bpyPEG_2$ to iron(II) sulfate loadings ($[FeSO_4]_0 = {}^1/_3[bpyPEG_2] \sim 80\ \mu M$) were performed in aqueous solution under ambient atmosphere and monitored over time (Figure 4; Table 3). Polymeric iron complexes of similar molecular weights made from macroligands prepared by different methods typically exhibit comparable rates of formation and extinction coefficients

Table 3. Kinetics Data for $[Fe(bpyPEG_2)_3]SO_4$ Formation and Decay under Air[a]

			formation		decay			
entry	ligand	M_n	time[b] (min)	ϵ[c] (M^{-1} cm^{-1})	onset[d] (h)	k[e] (h^{-1})	$t_{1/2}$ (h)	A'/A_{max}[f] ($\times$ 100)
1	bpy	156	<1	8250				
2	bpy + PEG	4600	<1	8150	0.083	0.026	26.7	0
3	$bpy(PEGOCH_3)_2$	4100	15	9290	1.7	0.076	9.1	8
4	$bpyPEG_2$[g]	5300	15	9740	0.9	0.071	9.8	8
5	$bpyPEG_2$[h]	5300	<30	9840	0.5	0.070	9.9	12
6	$bpyPEG_2$	6200	15	8690	2.5	0.098	7.1	2
7	$bpyPEG_2$	11600	50	7470	4.0	0.115	6.0	0
8	$bpyPEG_2$[i]	17400	53	6740	7.1	0.151	4.6	11

[a] Reaction conditions: $[FeSO_4]_0 = {}^1/_3[\text{bpy ligand}]_0 = 80$ μM in H_2O at room temperature with exposure to air and light unless otherwise indicated. [b] Approximate time required to reach maximum absorbance at MLCT λ_{max} (i.e., 522 nm for bpy; ~532 nm for $bpyPEG_2$). [c] Extinction coefficient determined at maximum absorbance. [d] Time after which the absorbance begins to drop (see Figure 4). [e] Rate constant for the disappearance of Fe(II) tris(bpy) species determined from the decrease in absorbance at MLCT λ_{max} ($[Fe(bpyPEG_2)_3]^{2+}$, ~532 nm; $[Fe(bpy)_3]^{2+}$ + PEG, 522 nm). Note that $[Fe(bpy)_3]^{2+}$ is stable under these conditions. [f] Residual absorbance after decay (A') expressed as a percentage of maximum absorbance reached before decay (A_{max}). [g] Data for ϵ, decay onset, and k are presented as averages of three runs (standard deviation: $\epsilon = 196$, decay onset 0.2, $k = 0.013$, $A' = 5$). [h] Performed in the dark. Data were collected every 30 min throughout the experiment. Data for ϵ and k are presented as averages of three runs (standard deviation: $\epsilon = 90$, $k = 0.011$, $A' = 5$). [i] Data are presented as averages of five runs (standard deviation: formation = 8, $\epsilon = 144$, decay onset 5.8, $k = 0.027$, $A' = 5$).

(i.e., Table 3, coupling, entry 3; different hydroxyl:base loadings, 1:0.35, entry 4, and 1:0.5, entry 6). Extinction coefficients given in Table 3 are comparable to those calculated at the titration end points in Table 2 (i.e., within ~10%). For low molecular weight $[Fe(bpyPEG_2)_3]^{2+}$ complexes that form efficiently, extinction coefficients are slightly higher than that of $[Fe(bpy)_3]^{2+}$ (compare entries 1 and 2−4). However, molecular weight effects are observed. Times required for solutions to reach maximum absorbance increase with macroligand molecular weight, whereas extinction coefficients typically decrease (i.e., Table 3: for $M_n = 5300$, ~15 min and $\epsilon = 9740$ M^{-1} cm^{-1}; for $M_n = 17\,400$, ~1 h and $\epsilon = 6740$ M^{-1} cm^{-1}). Similar molecular weight effects have been observed previously for iron chelation to other macroligands; however, the molecular weight range over which they occur is more compressed for PEG, and coordination reactions with PEG are typically slower than other polymeric bpy ligands of comparable and even higher molecular weights.[42,44,59]

While lower extinction coefficients may suggest something about the quality of higher molecular weight $bpyPEG_2$ samples, they could also signal differences in the extent of formation of the iron tris(bpy) complexes or their stability. The fact that absorbances measured at λ_{max} tend to plateau at maximum values before decay commences suggests that, even for high molecular weight samples, equilibration occurs and thermodynamic products are attained. Hence, assuming that higher molecular weight samples have the targeted structure and composition, low extinction coefficients may be due to less tris product at equilibrium rather than to degradation concomitant with product formation. Though other iron(II) bpy species could be present, normally mono and bis species of nonpolymeric iron(II) bpy complexes exist only in extremely small amounts in aqueous solutions due to the high formation constant of the iron tris(bpy) species ($K_3 \gg K_2$ and K_1). This deviation from the normal statistical relationship (i.e., $K_1 > K_2 > K_3$) stems from the increased stability of the low-spin tris(bpy) complex relative to labile, high-spin mono and bis complexes. Under special circumstances mono and bis complexes can be observed, however. For example, under strongly acidic conditions in the presence of a large excess of Fe^{2+}, high-spin mono bpy complexes can form ($\lambda_{max} = 435$ nm, $\epsilon = 310$ M^{-1} cm^{-1}),[65] and bis bpy complexes with anionic ligands, $Fe(bpy)_2(X)_2$ ($X^- = CN^-$, SCN^-, or Cl^-), have also been reported;[66] however, these conditions do not apply to the $[Fe(bpyPEG_2)_3]^{2+}$ reactions unless sulfate is a non-innocent counter-ion. Perhaps more relevant to the PEG case is the ready solvolysis of $[Fe(bpy)_3]^{2+}$ in neutral polar aprotic solvents such as *N*,*N*-dimethylformamide (DMF) or DMSO to form dicationic iron bis(bpy) solvento complexes. For DMF, a high- to low-spin transition occurs between mono and bis complexes (i.e., $K_1 < K_2 > K_3$), not bis and tris as is noted for iron(II) bpy complexes in aqueous solution. The absorption spectrum for low-spin $[Fe(bpy)_2(DMF)_2]^{2+}$ resembles that of the iron tris bpy complex but with lower extinction coefficients, particularly in the visible region.[67] The ways in which aqueous PEG environments affect the formation, stability, and spectral properties of the mono and bis bpy ferrous intermediates is not known. However, these prior reports suggest that if high-spin $[Fe(bpy)X_n]^{2+}$ or $[Fe(bpy)_2X_m]^{2+}$ complexes are present (X = H_2O, PEG ethers), they are not expected to interfere with analysis of the disappearance of the tris bpy chromophore at $\lambda_{max} = 530$ nm. If low-spin bis(bpy) complexes are present, they could be difficult to distinguish from tris complexes by UV−vis spectroscopy other than by their depressed extinction coefficients.

When solutions were monitored beyond the point where maximum absorbance was reached, it was discovered that polymeric iron tris($bpyPEG_2$) complexes were unstable over time. Similar but slower degradation was also noted for a control reaction involving Fe^{2+}, bpy, and PEG ($M_n = 4600$) (Figure 4). (No significant differences were noted when $[Fe(bpy)_3]^{2+}$ was formed in situ in the presence of PEG versus addition of PEG to preformed $[Fe(bpy)_3]^{2+}$.) Selected UV−vis spectra recorded during the formation and disappearance of an iron complex prepared from $bpyPEG_2$ ($M_n = 6200$) are presented in Figure 5, along with the spectrum of the corresponding $bpyPEG_2$ macroligand for comparison. No clean isosbestic points are noted in spectral overlays representative of the entire course of the reactions (data not shown), suggesting that multistep processes may be operative. The onset of degradation of polymeric iron complexes varies from sample to sample and was not always reproducible from run to run for a given sample. This variation was most dramatic for complexes made from high molecular weight $bpyPEG_2$ ($M_n = 17\,400$), which began to degrade after 1.5, 3, 6, 9, and 16 h in experiments performed by the same method. However, regardless of the onset time, once degradation under air commenced, the rates of disappearance of iron tris($bpyPEG_2$) chromophores (i.e., drop in absorbance at λ_{max} ~532 nm) are typically quite reproducible from run to run for a given sample.

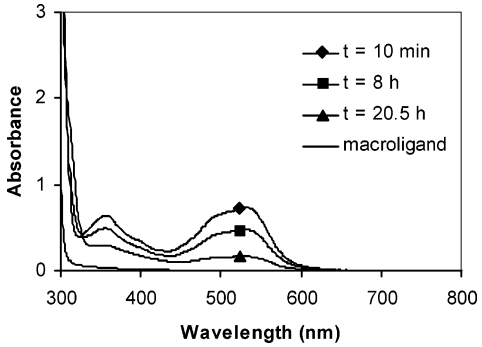

Figure 5. UV−vis spectra of a bpyPEG$_2$ macroligand (M_n = 6200) and the corresponding $[Fe(bpyPEG_2)_3]^{2+}$ complex in water under ambient atmosphere monitored over time.

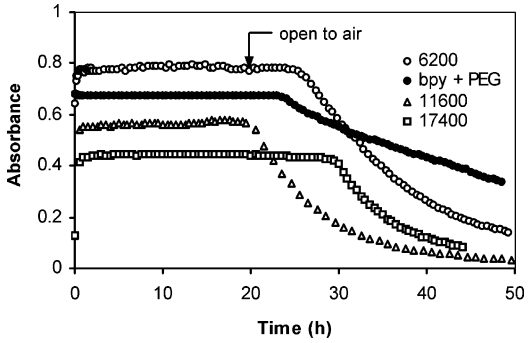

Figure 6. Rate comparison of $[Fe(bpyPEG_2)_3](SO_4)$ complex formation in water under argon followed (after 20 h) by degradation under air for samples prepared from bpyPEG$_2$ macroligands of different molecular weights (M_n = 6200, 11 600, and 17 400). Formation and degradation of $[Fe(bpy)_3](SO_4)$ in the presence of PEG (M_n = 4600) is provided for comparison. ($[FeSO_4]_0 = {}^1/_3[bpy\ ligand]_0 = 80\ \mu M$; absorbance changes were monitored at MLCT $\lambda_{max} \sim 532$ nm for bpyPEG$_2$ macroligands and 522 nm for bpy.)

Generally, the absorbance at $\lambda_{max} \sim 532$ nm (A_{max}) reaches a minimal value (A') over time. For reactions run in air, the residual value, A', ranges from ~0−12% of A_{max} (Table 3). Similar behavior was noted for $[Fe(bpyPEG_2)_3]^{2+}$ in phosphate-buffered saline solution. This may suggest that a new equilibrium is established between $[Fe(bpyPEG_2)_3]^{2+}$ and other iron species in solution [e.g., Fe(II) bis(bpy) or oxidized iron complexes]. However, absorbances associated with $[Fe(bpy)_3]^{3+}$ {λ_{max}, nm (ϵ, $M^{-1}\ cm^{-1}$) = 610 (300), 520 (108), 390 (1210), and 218 (6.9×10^4)}[68] are not evident in the UV−vis spectra of solutions after degradation (e.g., see Figure 5). Reduction of iron(III) hydroxides to generate iron(II) and hydroxyl radicals is known for aqueous solutions exposed to light.[69] The extent to which such a photochemical process might be operative here is not known. Addition of 3 equivalents of bpy to a degraded solution of $[Fe(bpyPEG_2)_3]^{2+}$, in an attempt to shift iron species to the Fe(II) tris bpy complexes, resulted in only a very slight increase of absorbance at λ_{max} = 532 nm (degraded solution, A/A_{max} = 0.31; after addition of bpy, A/A_{max} = 0.39).

For the data analysis, both pseudo−first-order and second-order reaction expressions were tested to fit the rate of disappearance of iron tris(bpyPEG$_2$). An absorbance offset (A') was added to the equations to represent the residual value reached after decay. The exponential model ($A = A' + A_0e^{-kt}$) fits the data best with $\chi^2 \sim 10^{-4}$, which is smaller than the error observed for the second-order rate equation. Rate constants and half-lives for the disappearance of iron tris(bpyPEG$_2$) are given in Table 3, showing that low molecular weight iron-centered star polymers degrade more slowly than higher molecular weight samples under comparable conditions. Similar trends in rates of decay and extinction coefficients were observed with another iron salt, $Fe(NH_4)_2(SO_4)_2$ (for bpyPEG$_2$ M_n = 5300, k = 0.064 h^{-1} and ϵ = 9922 $M^{-1}\ cm^{-1}$; for M_n = 11 600, k = 0.137 h^{-1} and ϵ = 8014 $M^{-1}\ cm^{-1}$). Although an impurity from the macroligand synthesis may be responsible for this degradation behavior, this seems unlikely because bpyPEG$_2$ samples prepared by different synthetic methods (e.g., Table 3: coupling, entry 3; anionic polymerization, entry 4) degrade similarly upon iron chelation. Furthermore, filtration of PEG through alumina in an attempt to remove other impurities just prior to use in control reactions with Fe^{2+} and bpy showed no measurable effect on the rate data obtained.

Aqueous solutions of ferrous salts can undergo oxidation with concomitant generation of reactive oxygen species. For example, peroxide impurities in the PEG or generated in situ could lead to Fenton chemistry.[70] Chelating ligands can sometimes prevent or at least reduce the formation of radicals; however, the nature and the size of the ligand as well as the solvent environment can affect the reactivity of iron.[41,71] Previously, iron bpy complexes and O_2 have been utilized for alkene and alkyl benzene oxygenation.[72] Though no measurable degradation was observed for $[Fe(bpy)_3]^{2+}$ solutions under air over the course of weeks or more, we were nonetheless curious whether O_2 might be functioning as an oxidant in the decomposition of the polymeric complexes, $[Fe(bpyPEG_2)_3]^{2+}$. Indeed, when reactions were run under argon, the resulting polymeric Fe tris(bpy) complexes were stable (Figure 6; Table 4). When UV−vis cuvettes were opened to air after ~20 h, absorbances at λ_{max} = 532 nm ultimately decreased at rates comparable to what was observed for samples prepared under ambient atmosphere. Here, the residual absorbance A' ranges from ~1−4% of A_{max} (Table 4). Similar molecular weight trends were noted and a pseudo-first-order rate law again applies. For Fe/bpy/PEG control reactions run under comparable conditions and monitored at λ_{max} = 522 nm, similar phenomena are noted (Figure 6; Table 4, entry 1).

Some reactions involving iron salts in aqueous solution are promoted by light, and previously, light-sensitive chemistry was noted for iron complexes with certain poly(acrylate)-based bpy macroligands in preliminary studies.[73] In contrast to Ru or Os, photoexcited $[Fe(bpy)_3]^{2+}$ does not typically activate molecular oxygen via a bimolecular mechanism because the excited states of the complex are very short-lived.[46,74] However, photoexcitation of $[Fe(bpy)_3]^{2+}$ immobilized on Amberlite resin has been utilized to activate O_2 for the degradation of organic dyes such as rhodamine B. On the basis of electron paramagnetic resonance (EPR) and chemical tests for singlet oxygen and hydroxyl or hydroperoxyl radicals, superoxide and iron oxo species were proposed for this organic pollutant detoxification process.[46−48] To test whether light plays a role in the degradation of $[Fe(bpyPEG_2)_3]^{2+}$, 3:1 mixtures of bpyPEG$_2$ to Fe^{2+} were combined in aqueous solution in air and were monitored over time with light strictly excluded. Extinction coefficients and rate constants for decomposition were comparable to those for reactions run in the presence of light. Thus, at least for the conditions tested, light does not appear to be a factor in the reactivity observed for iron tris(bpyPEG$_2$) complexes.

Though we have yet to detect reactive oxygen species that may be generated by reaction of O_2 or peroxides with $[Fe(bpyPEG_2)_3]^{2+}$ samples, circumstantial evidence suggests that radicals may be involved. An aqueous solution of $[Fe(bpyPEG_2)_3]^{2+}$ prepared from bpyPEG$_2$ (M_n = 15 900, PDI = 1.12) was allowed to stand for 40 days in a sealed vial under air. GPC analysis after this time showed significant degradation

Table 4. Kinetics Data for Formation of $[Fe(bpyPEG_2)_3]SO_4$ under Argon and Decay of the Polymeric Complex Once Opened to Air[a]

		formation		decay		
entry	$bpyPEG_2$ M_n	time[b] (min)	ϵ[c] (M^{-1} cm^{-1})	k[d] (h^{-1})	$t_{1/2}$ (h)	A'/A_{max}[e] ($\times$ 100)
1	bpy + PEG[f]	1	8490	0.029	23.9	8
2	5300	<30	9144	0.059	11.7	4
3	6200	20	8622	0.076	9.1	1
4	11 600	40	7195	0.123	5.6	3
5	17 400	60	6190	0.188	3.7	2

[a] Reaction conditions: $[FeSO_4]_0 = {}^1/_3[\text{bpy ligand}]_0 = 80\ \mu M$ in H_2O at room temperature with exposure to light. Reactions were run under argon for 20 h and then were opened to air. [b] Approximate time required to reach maximum absorbance a MLCT λ_{max} ~532 nm (522 nm for entry 1). [c] Extinction coefficient determined at maximum absorbance. [d] Rate constant for the disappearance of Fe(II) tris(bpy) species determined from the decrease in absorbance at MLCT, λ_{max} ($[Fe(bpyPEG_2)_3]^{2+}$, ~532 nm; $[Fe(bpy)_3]^{2+}$ + PEG, 522 nm). [e] Residual absorbance after decay (A') expressed as a percentage of maximum absorbance reached before decay (A_{max}). [f] M_n = 4600, PDI = 1.05.

of the polyether chains, as evidenced by a drop in molecular weight and a broadening of the molecular weight distribution (M_n = 6200, PDI = 1.57) compared to an aqueous solution of the corresponding $bpyPEG_2$ treated similarly (M_n = 14 800, PDI = 1.14). [Note: Iron tris($bpyPEG_2$) complexes fragment into their component macroligands on the GPC columns. Molecular weights measured for the degraded iron stars likely correspond to the degraded macroligands.] Previous reports also describe the degradation of PEG in the presence of metal ions; radical mechanisms are often invoked.[75−77]

Furthermore, $bpyPEG_2$ modified with methacrylate groups at the hydroxyl chain ends [i.e., bpy(PEG-OC(O)C(CH_3)=CH_2)$_2$, bpy(PEG-MA)$_2$] spontaneously cross-linked to form pink hydrogels upon exposure to aqueous solutions of ferrous salts.[78] As the previous kinetics and titration studies illustrate, when a comparable quantity of an iron salt is combined with $bpyPEG_2$ (bearing OH not methacrylate end groups) in aqueous solution, soluble polymeric metal complexes form, not gels. In the absence of iron, bpy(PEG-MA)$_2$ does not form a gel in aqueous solution either. Ordinarily, radical initiators are required to form hydrogels from PEG acrylates.[79,80] These observations also point to the possibility of radical species in the $[Fe(bpyPEG_2)_3]^{2+}$ reaction mixtures.

Synthesis of $[Fe(bpyPEG_2)_3]SO_4$. With results from titration and kinetics analyses as a starting point, a preparative-scale synthesis of $[Fe(bpyPEG_2)_3]SO_4$ was performed. A polymeric iron complex was formed in aqueous solutions under argon, concentrated in vacuo and isolated by precipitation from CH_2Cl_2 into cold diethyl ether. The resulting red-violet powder was characterized spectrophotometrically in aqueous solution under air and showed the typical absorbance for $[Fe(bpyPEG_2)_3]^{2+}$ at λ_{max} (MLCT) = 531 nm (ϵ = 9420 M^{-1} cm^{-1}).

Conclusion

This study involving iron complexes with water-soluble $bpyPEG_2$ macroligands has raised a number of issues that are important to consider when metals are combined with polymers for biomaterials applications. First, macroligand syntheses must be optimized. For $bpyPEG_2$ formed by anionic polymerization, the base to initiator loading can affect the solubility of the activated initiator and the quality of the polymeric ligand that results. Polydispersities are lower when substoichiometric loadings of base to hydroxyl initiator sites are utilized. Second, chelation and titration studies are good ways to test macroligand quality. Typically, extinction coefficients for polymeric iron tris(bpy) complexes are slightly higher than those for the parent $[Fe(bpy)_3]^{2+}$ measured under similar conditions. If these values are not comparable, this may indicate a potential problem with the macroligand or signal complex instability. Similarly, if 3:1 macroligand-to-metal ratios are obtained in titration experiments, a common method for polymer end-group determination, this helps to verify that $bpyPEG_2$ samples possess the requisite number of bpy binding sites per chain. Third, many polymer chains possess Lewis basic sites (e.g., oxygen donors on PEG) that can compete with tailored metal binding sites on macroligands (e.g., bpy). This may explain why coordination of iron to $bpyPEG_2$ is slow relative to other kinds of polymeric ligands of comparable and even higher molecular weight. However, for iron chelation to $bpyPEG_2$ and control reactions involving bpy and PEG, iron tris(bpy) complexes ultimately form. Fourth, it is important to test and monitor the stability of the iron salts and complexes in different solvent systems over time, since polymeric complexes can exhibit different reactivities than their nonpolymeric counterparts. Here we report air sensitivity for Fe $bpyPEG_2$ complexes and $[Fe(bpy)_3]^{2+}$/PEG mixtures under conditions where $[Fe(bpy)_3]^{2+}$ is stable. Finally, molecular weight effects are manifested in a number of different ways. The time required to form tris complexes increases with molecular weight, whereas the extent of product formation decreases. Higher molecular weight metal-centered stars may be less stable thermodynamically, as evidenced by less iron tris(bpy) product at equilibrium. (This assumes that samples are of similar quality and that differential error in molecular weight measurement is not operative for macroligands of different sizes.) Additionally, the rates of disappearance of higher molecular weight Fe tris($bpyPEG_2$) complexes are faster than low molecular weight complexes, once degradation commences under ambient atmosphere. Degradation is even slower when $[Fe(bpy)_3]^{2+}$ and PEG are not covalently attached. This may be due to differences in complex stability or in the rates of diffusion of oxygen[81] or other reactive species in the polymeric environments. A more thorough understanding of the reactivity of $[Fe(bpyPEG_2)_3]^{2+}$ systems in aqueous solution requires detailed characterization of magnetic and spectroscopic changes occurring at the iron center, identification of the reactive species (e.g., dioxygen, superoxide, peroxy or hydroxyl radicals, iron oxo complexes, etc) and polymer degradation products, and investigation of the reactivity in biological and environmental contexts. These studies serve as the subjects of future reports, which will enhance fundamental understanding and advance our goals of adapting these responsive biomaterials for practical uses.

Acknowledgment. We gratefully acknowledge the National Science Foundation (BES-042212, CHE-0350121), the American Cancer Society, and the Commonwealth Health Research Board for support for this work. Drs. Timothy Wedge and Robert M. Johnson are also thanked for their assistance.

References and Notes

(1) (a) Manners, I. *Synthetic Metal-Containing Polymers*; Wiley−VCH: Weinheim, Germany, 2004. (b) Wöhrle, D.; Pomogailo, A. D. *Metal Complexes and Metals in Macromolecules*; Wiley−VCH: Weinheim, Germany, 2003.

(2) Fraser, C. L.; Smith, A. P. *J. Polym. Sci., Part A: Polym. Chem.* **2000**, *38*, 4704.

(3) Schubert, U. S.; Eschbaumer, C. *Angew. Chem., Int. Ed.* **2002**, *41*, 2892.

(4) Pollino, J. M.; Weck, M. *Chem. Soc. Rev.* **2005**, *34*, 193.

(5) Shenhar, R.; Norsten, T. B.; Rotello, V. M. *Adv. Mater.* **2005**, *17*, 657.

(6) Hofmeier, H.; Schubert, U. S. *Chem. Commun.* **2005**, *19*, 2423.

(7) (a) Hjelm, J.; Handel, R. W.; Hagfeldt, A.; Constable, E. C.; Housecroft, C. E.; Forster, R. J. *Inorg. Chem.* **2005**, *44*, 1073. (b) Gould, S.; Strouse, G. F.; Meyer, T. J.; Sullivan, B. P. *Inorg. Chem.* **1991**, *30*, 2942.

(8) (a) Higley, M. N.; Pollino, J. M.; Hollenbeak, E.; Weck, M. *Chem. Eur. J.* **2005**, *11*, 2946. (b) Hofmeier, H.; Hoogenboom, R.; Wouters, M. E. L.; Schubert, U. S. *J. Am. Chem. Soc.* **2005**, *127*, 2913.

(9) Ogoshi, T.; Itoh, H.; Kim, K.-M.; Chujo, Y. *Macromolecules* **2002**, *35*, 334.

(10) For examples, see Beck, J. B.; Ineman, J. M.; Rowan, S. J. *Macromolecules* **2005**, *38*, 5060 and references therein.

(11) Andres, P. R.; Schubert, U. S. *Adv. Mater.* **2004**, *16*, 1043.

(12) (a) Li, M.; Mann, S. *J. Mater. Chem.* **2004**, *14*, 2260. (b) Arvizo, R. R.; Verma, A.; Rotello, V. M. *Supramol. Chem.* **2005**, *17*, 155. (c) Hofmeier, H.; Pahnke, J.; Weidl, C. H.; Schubert, U. S. *Biomacromolecules* **2004**, *5*, 2055. (d) Torchilin, V. *Bioconjugate Chem.* **1999**, *10*, 146.

(13) (a) Bender, J. L.; Corbin, P. S.; Fraser, C. L.; Metcalf, D. H.; Richardson, F. S.; Thomas, E. L.; Urbas, A. M. *J. Am. Chem. Soc.* **2002**, *124*, 8526. (b) Park, C.; McAlvin, J. E.; Fraser, C. L.; Thomas, E. L. *Chem. Mater.* **2002**, *14*, 1225.

(14) Fustin, C.-A.; Lohmeijer, B. G. G.; Duwez, A.-S.; Jonas, A. M.; Schubert, U. S.; Gohy, J.-F. *Adv. Mater.* **2005**, *17*, 1162.

(15) Zhou, G.; Harruna, I. I. *Macromolecules* **2005**, *38*, 4114.

(16) For example, see Mann, S. *Chem. Commun.* **2004**, *1*, 1.

(17) (a) Zimmermann, N.; Meggers, E.; Schultz, P. G. *J. Am. Chem. Soc.* **2002**, *124*, 13684. (b) Atwell, S.; Meggers, E.; Spraggon, G.; Schultz, P. G. *J. Am. Chem. Soc.* **2001**, *123*, 12364.

(18) Popescu, D.-L.; Parolin, T. J.; Achim, C. *J. Am. Chem. Soc.* **2003**, *125*, 6354.

(19) (a) Wang, C.; Stewart, R. J.; Kopecek, J. *Nature* **1999**, *397*, 417. (b) For a related example, see Xu, C.; Breedveld, V.; Kopecek, J. *Biomacromolecules* **2005**, *6*, 1739.

(20) Tor, Y. *C. R. Chim.* **2003**, *6*, 755.

(21) For example, see (a) Gorczynski, J. L.; Chen, J.; Fraser, C. L. *J. Am. Chem. Soc.* **2005**, *127*, 14956. (b) McAlvin, J. E.; Scott, S. B.; Fraser. C. L. *Macromolecules* **2000**, *33*, 6953.

(22) For an interesting example of a temperature-sensitive metallopolymer, see Beck, J. B.; Rowan, S. J. *J. Am. Chem. Soc.* **2003**, *125*, 13922.

(23) Zhao, Y.; Beck, J. B.; Rowan, S. J.; Jamieson, A. M. *Macromolecules* **2004**, *37*, 3529.

(24) (a) Clarke, Y.; Xu, W.; Demas, J. N.; DeGraff, B. A. *Anal. Chem.* **2000**, *72*, 3468. (b) Bare, W. D.; Mack, N. H.; Xu, W.; Demas, J. N.; DeGraff, B. A. *Anal. Chem.* **2002**, *74*, 2198. (c) Parker, D.; Senanayake, K.; Williams, J. A. G. *Chem. Commun.* **1997**, *18*, 1777.

(25) (a) Haskins-Glusac, K.; Pinto, M. R.; Tan, C.; Schanze, K. S. *J. Am. Chem. Soc.* **2004**, *126*, 14964. (b) Han, B.-H.; Manners, I.; Winnik, M. A. *Chem. Mater.* **2005**, *17*, 3160.

(26) (a) Wang, J.; Luthey-Schulten, Z. A.; Suslick, K. S. *Proc. Natl. Acad. Sci.* **2003**, *100*, 3035. (b) Suslick, K. S.; Rakow, N. A.; Sen, A. *Tetrahedron* **2004**, *60*, 11133.

(27) Demas, J. N.; DeGraff, B. A. *Coord. Chem. Rev.* **2001**, *211*, 317.

(28) Fraser, C. L.; Smith, A. P. *Comprehensive Coordination Chemistry II*; Meyer, T. J., McCleverty, J. A., Eds; Elsevier Ltd.: Oxford, U.K., 2004; Vol. 1, Chapt. 1, pp 1−23.

(29) *Poly(ethylene glycol) Chemistry and Biological Applications*; Harris, J. M., Zalipsky, S. Eds.; ACS Symposium Series 680; American Chemical Society: Washington, DC, 1997.

(30) (a) Mrksich, M.; Whitesides, G. M. *Annu. Rev. Biophys. Biomol. Struct.* **1996**, *25*, 55. (b) Nath, N.; Hyun, J.; Ma, H.; Chilkoti, A. *Surf. Sci.* **2004**, *570*, 98.

(31) (a) Duncan, R. *Nat. Rev.* **2003**, *2*, 347. (b) Uhrich, K. E.; Cannizzaro, S. M.; Langer, R. S.; Shakesheff, K. M. *Chem. Rev.* **1999**, *99*, 3181.

(32) Allen, T. M.; Cullis, P. R. *Science* **2004**, *303*, 1818.

(33) (a) Hubbell, J. A. *Curr. Opin. Biotechnol.* **2003**, *14*, 551. (b) Levenberg, S.; Langer, R. *Curr. Top. Dev. Biol.* **2004**, *61*, 113.

(34) Roberts, M. J.; Bentley, M. D.; Harris, J. M. *Adv. Drug Delivery Rev.* **2002**, *54*, 459.

(35) (a) Long, J. W.; Velazquez, C. S.; Murray, R. W. *J. Phys. Chem.* **1996**, *100*, 5492. (b) Chujo, Y.; Naka, A.; Kraemer, M.; Sada, K.; Saegusa, T. *J. Macromol. Sci., Pure Appl. Chem.* **1995,** *A32*, 1213. (c) Naka, K.; Kobayashi, A.; Chujo, Y. *Macromol. Rapid Commun.* **1997**, *18*, 1025. (d) Marin, V.; Holder, E.; Meier, M. A. R.; Hoogenboom, R.; Schubert, U. S. *Macromol. Rapid Commun.* **2004**, *25*, 793.

(36) Schmatloch, S.; van den Berg, A. M. J.; Alexeev, A. S.; Hofmeier, H.; Schubert, U. S. *Macromolecules* **2003**, *36*, 9943.

(37) (a) Zalipsky, S. *Bioconjugate Chem.* **1995**, *6*, 150. (b) Akiyama, Y.; Otsuka, H.; Nagasaki, Y.; Kato, M.; Kataoka, K. *Bioconjugate Chem.* **2000**, *11*, 947.

(38) Lee, Y.; Koo, H.; Jin, G.; Mo, H.; Cho, M. Y.; Park, J.-Y.; Choi, J. S.; Park, J. S. *Biomacromolecules* **2005**, *6*, 24.

(39) For examples of responsive materials, see (a) Rehor, A.; Hubbell, J. A.; Tirelli, N. *Langmuir* **2005**, *21*, 411. (b) Kost, J.; Langer, R. *Adv. Drug Delivery Rev.* **2001**, *46*, 125. (c) Jeong, B.; Kim, S. W.; Bae, Y. H. *Adv. Drug Delivery Rev.* **2002**, *54*, 37.

(40) Langer, R.; Tirrell, D. A. *Nature* **2004**, *428*, 487 and examples therein.

(41) Hawker, P. N.; Twigg, M. V. In *Comprehensive Coordination Chemistry*; Wilkinson, G., Ed.; Pergamon Press: Oxford, U.K., 1987; Vol. 4, pp 1214−9.

(42) Johnson, R. M.; Pfister, A.; Fraser, C. L. in *Metal-Containing and Metallo-Supramolecular Polymers and Materials*; Newkome, G. R., Manner, I., Schubert, U. S., Eds.; ACS Symposium Series; American Chemical Society: Washington, DC, 2005; in press.

(43) (a) Schaggar, R. S.; Hall, A. J.; Miller, J. D. *Polymer* **1996**, *37*, 5313. (b) Viau, L.; Even, M.; Maury, O.; Haddleton, D. M.; Le Bozec, H. *Macromol. Rapid Commun.* **2003**, *24*, 630. (c) Chujo, Y.; Sada, K.; Saegusa, T. *Macromolecules* **1993**, *26*, 6315. (d) Card, R. J.; Neckers, D. C. *Inorg. Chem.* **1978**, *17*, 2345.

(44) Johnson, R. M.; Fraser, C. L. *Macromolecules* **2004**, *37*, 2718.

(45) (a) Groves, J. T. *Proc. Natl. Acad. Sci. U.S.A.* **2003**, *100*, 3569. (b) Halliwell, B.; Gutteridge, J. M. C. *Free Radicals in Biology and Medicine*, 3rd ed.; Oxford University Press: Oxford, U.K., 1999.

(46) Ma, W.; Li, J.; Tao, X.; He, J.; Xu, Y.; Yu, J. C.; Zhao, J. *Angew. Chem., Int. Ed.* **2003**, *42*, 1029.

(47) Li, J.; Ma, W.; Huand, Y.; Tao, X.; Zhao, J.; Xu, Y. *Appl. Catal. B: Environ.* **2004**, *48*, 17.

(48) Li, J.; Ma, W.; Huang, Y.; Cheng, M.; Zhao, J.; Yu, J. C. *Chem. Commun.* **2003**, 2214.

(49) Smith, A. P.; Corbin, P. S.; Fraser, C. L. *Tetrahedron Lett.* **2000**, *41*, 2787.

(50) Jiang, Y. X.; Song, W. B., Liu, Y.; Wei, B.; Cao, X. C.; Xu, H. D. *Mater. Chem. Phys.* **2000**, *62*, 109.

(51) Smith, A. P.; Fraser, C. L. *Macromolecules* **2003**, *36*, 2654.

(52) Pangborn, A. B.; Giardello, M. A.; Grubbs, R. H.; Rosen, R. K.; Timmers, F. J. *Organometallics* **1996**, *15*, 1518.

(53) Yasuji, K.; Nakamura, T.; Nagasaki, Y.; Kato, M.; Kataoka, K. *Macromolecules* **1999**, *32*, 8024.

(54) Hillmyer, M. A.; Bates, F. S. *Macromolecules* **1996**, *29*, 6994.

(55) Goddu, R. F.; Hume, D. N. *Anal. Chem.* **1954**, *26*, 1740.

(56) Knischka, R.; Lutz, P. J.; Sunder, A.; Mülhaupt, R.; Frey, H. *Macromolecules* **2000**, *33*, 315.

(57) Angot, S.; Taton, D.; Gnanou, Y. *Macromolecules* **2000**, *33*, 5418.

(58) Reed, N. N.; Janda, K. D. *J. Org. Chem.* **2000**, *65*, 5843.

(59) Corbin, P. S.; Webb, M. P.; McAlvin, J. E.; Fraser, C. L. *Biomacromolecules* **2001**, *2*, 223.

(60) To test the stability of the iron salt in water over time, the iron stock solution was retitrated with bpy after its use in bpyPEG_2 titration studies. After it stood in air for ~6.5 h there was no detectable change in the concentration of iron(II) in the stock solution. However, titration of the iron stock solution with bpy after 1 day under ambient conditions indicates some loss of Fe(II) (86% of original amount). Thus, iron solutions were freshly prepared and titrated for each experiment.

(61) (a) Bernson, A.; Lindgren, J.; Huang, W.; Frech, R. *Polymer* **1995**, *36*, 4471. (b) Caminiti, R.; Carbone, M.; Panero, S.; Sadun, C. *J. Phys. Chem. B* **1999**, *103*, 10348.

(62) (a) Wu, X.; Fraser, C. L. *Macromolecules* **2000**, *33*, 4053. (b) Wu, X.; Fraser, C. L. *Macromolecules* **2000**, *33*, 7776.
(63) (a) Hill, R. *Proc. R. Soc. (London)* **1930**, *B107*, 205. (b) Moss, M. L.; Mellon, M. G. *Ind. Eng. Chem., Anal. Ed.* **1942**, *14*, 862. (c) Alexander, R. D.; Buisson, D. H.; Dudeney, W. L.; Irving, R. J. *J. Chem. Soc., Faraday Trans. 1: Phys. Chem. Condensed Phases* **1978**, *74*, 1081.
(64) Aqueous solutions of $[Fe(bpy)_3](SO_4)$ exposed to air were stable after a month when monitored by UV−vis spectroscopy.
(65) Krumholz, P. *J. Am. Chem. Soc.* **1949**, *71*, 3654.
(66) Blandamer, M. J.; Burgess, J.; Chambers, J. G. *J. Chem. Soc., Dalton Trans.* **1976**, 606.
(67) Josceanu, A. M.; Moore, P. *J. Chem. Soc., Dalton Trans.* **1998**, 369.
(68) Nord, G.; Pedersen, B.; Bjergbakke, E. *J. Am. Chem. Soc.* **1983**, *105*, 1913.
(69) Szacilowski, K.; Macyk, W.; Drzewiecka-Matuszek, A.; Brindell, M.; Stochel, G. *Chem. Rev.* **2005**, *105*, 2647.
(70) (a) Wardman, P.; Candeias, L. P. *Radiat. Res.* **1996**, *145*, 523. (b) Liochev, S. I. In *Metal Ions in Biological Systems*; Sigel, A., Sigel, H., Eds.; Marcel Dekker: New York, 1999; Vol. 36, pp 1−39.
(71) Welch, K. D.; Davis, T. Z.; Aust, S. D. *Arch. Biochem. Biophys.* **2002**, *397*, 360.
(72) (a) Sobkowiak, A.; Narog, D.; Sawyer, D. T. *J. Mol. Catal. A: Chem.* **2000**, *159*, 247. (b) Lei, Z.-Q.; Wang, Y.-P. *React. Polym.* **1992**, *16*, 223.
(73) Johnson, R. M.; Fraser, C. L.; Turro, C. Unpublished results.
(74) Also see (a) Ferrere, S. *Chem. Mater.* **2000**, *12*, 1083. (b) Nguyen, T. H.; Shannon, P. J.; Hoggard, P. E. *Inorg. Chim. Acta* **1999**, *291*, 136.
(75) Brand, N.; Mailhot, G.; Bolte, M. *Chemosphere* **2000**, *40*, 395.
(76) Kaczmarek, H.; Rabek, F. *Angew. Makromol. Chem.* **1997**, *247*, 111.
(77) Duval, M.; Sarazin, D. *Macromolecules* **2003**, *36*, 1318.
(78) (a) For an interesting example of an oxygen-sensitive gelation reaction that is facilitated by Fenton chemistry, see Goessl, A.; Tirelli, N.; Hubbell, J. A. *J. Biomater. Sci., Polym. Ed.* **2004**, *15*, 895. (b) For a related example, see Napoli, A.; Valentini, M.; Tirelli, N.; Muller, M.; Hubbell, J. A. *Nat. Mater.* **2004**, *3*, 183.
(79) Sawhney, A.; Pathak, C. P.; Hubbell, J. A. *Macromolecules* **1993**, *26*, 581.
(80) Rydholm, A. E.; Bowman, C. N.; Anseth, K. S. *Biomaterials* **2005**, *26*, 4495.
(81) Fuller, Z. J.; Bare, W. D.; Kneas, K. A.; Xu, W.-Y.; Demas, J. N.; DeGraff, B. A. *Anal. Chem.* **2003**, *75*, 2670.

BM050652L